

Torque on a slip sphere rotating in a semi-infinite micropolar fluid

H. H. Sherief · M. S. Faltas · E. A. Ashmawy · M. G. Nashwan

Received: 15 November 2016 / Accepted: 24 January 2018 / Published online: 5 February 2018
© Springer Science+Business Media B.V., part of Springer Nature 2018

Abstract In this paper, the steady rotational motion of a slip sphere in a semi-infinite micropolar fluid is investigated. The sphere is assumed to rotate about a diameter perpendicular to an impermeable plane wall. The slip and spin boundary conditions are imposed on the spherical particle surface while on the plane wall surface the classical no-slip and no-spin conditions are utilized. A semi-analytical technique based on the principle of superposition together with a numerical method, called the collocation method, is employed to obtain the hydrodynamic torque acting on the spherical particle. Numerical results for the torque are obtained and illustrated graphically.

Keywords Micropolar fluid · Analytical–numerical technique · Collocation technique · Slip condition

1 Introduction

The Navier–Stokes theory cannot describe accurately the correct behavior of some types of fluids with microstructure. This motivated Eringen [1] to introduce his theory of micropolar fluids which give a mathematical model for many industrial and natural fluids appearing in biological sciences and engineering applications. The motion of a micropolar fluid is characterized by two main vectors: the classical velocity vector which describes the motion of macro-volume elements and the microrotation vector which is responsible for the rotation of microelements about their centroids in an average sense [1]. In the literature, there are several attempts to discuss the behavior of micropolar fluid flows under different boundary conditions. The axially symmetric micropolar fluid flow problems have recently attracted the attention of many researchers to investigate. A simple formula has been derived by Ramkissoon [2] to evaluate the couple experienced by a micropolar fluid on an axisymmetric body rotating slowly about its axis of symmetry. Charya and Iyengar have investigated the oscillatory flow of an approximated sphere rotating in a micropolar fluid in [3]. Sherief et al. [4] discussed the axi-symmetric motion of a general prolate body in a micropolar fluid. The couple experienced by axisymmetrical bodies rotating steadily in incompressible micropolar fluids is of practical interest in many technological applications. It is required for designing and calibrating viscometers that measure the viscosity

E. A. Ashmawy
Department of Mathematics and Computer Science,
Faculty of Science, Beirut Arab University, Beirut,
Lebanon

H. H. Sherief · M. S. Faltas · E. A. Ashmawy (✉) ·
M. G. Nashwan
Department of Mathematics and Computer Science,
Faculty of Science, Alexandria University, Alexandria,
Egypt
e-mail: emad_ashm@yahoo.com

coefficients of micropolar fluids [5]. This motivated the authors to investigate the rotational motion of axially symmetric bodies in steady incompressible micropolar fluid flows.

The study of interaction problems between small rigid particles and a wall has different practical applications in many fields such as separation processes and filtration, transport of sediments and motion of rigid cells in blood vessels. The interaction of a solid particle with a containing wall depends on the geometrical shape position, and orientation of the particle as well as the geometry of the wall. There are some studies in the literature that have treated the wall effects on the motion of a rigid particle relative to a wall over the past decades. Some authors have discussed the motion of a sphere translating along or rotating around an axis perpendicular or parallel to a smooth wall in a Stokes flow under the assumption of low Reynolds number, e.g. [6–8]. One of the efficient techniques used to treat this type of problems is a semi-analytical technique employing an efficient numerical method called the boundary collocation method. In this collocation method, the conditions imposed on the boundary are satisfied on the generating arc of the axisymmetric particle. These conditions result in a system of linear algebraic equations that could be solved simultaneously to give the desired unknown constants. Gluckman et al. [9] developed the technique of collocation series solution for unbounded, axially symmetric multi spherical Stokes flow. This work has been extended by Leichtberg et al. [10] to bounded flows for chains of coaxial spheres in tubes. A useful review of the use of the collocation method in mechanics can be found in [11]. The technique of collocation is also used by Ganatos et al. [12] to discuss the motion of a sphere in a viscous fluid normal to two parallel plane boundaries assuming no-slip condition. Keh and Chang [13] utilized the collocation technique to investigate the problem of creeping motion of a slip sphere perpendicular to two planar walls. Keh and Hsu [14] applied the same procedure to investigate the photophoretic motion of an aerosol sphere normal to a plane wall. For micropolar fluids, Kucaba-PiŃtal [15] applied the classical no-slip condition on the spherical boundary and on the wall to study the motion of a sphere normal to a plane wall.

The classical no-slip boundary condition has been used extensively in the field of fluid dynamics. However, in the last century various studies have

been demonstrated that the no-slip condition may not always occur and that the fluid particles may slip at the surface of the boundary [16–18]. There many research papers illustrate that the no-slip condition may lead to non realistic behavior; e.g. [19–22]. A general boundary condition that assumes that fluid particles are slipping on the solid boundary was proposed by Navier [23]. It assumes that the fluid tangential velocity relative to the solid boundary is proportional to the shearing stress acting at the contact point [24]. It has reported that, the slip condition has been applied to problems of Newtonian fluids [25–30] and recently of micropolar and microstretch fluids [31–34].

This work presents an analytical numerical treatment to the problem of the slow steady rotational motion of a micropolar fluid due to a rotation of a slip spherical particle about a diameter perpendicular to an impermeable plane wall. The spin and slip boundary conditions are used on the surface of the spherical particle while the classical no-slip and no-spin conditions are imposed on the wall. A semi analytical procedure based on the principle of superposition together with the numerical collocation technique is utilized.

2 Governing equations

The steady motion of a micropolar liquid, in the absence of body forces and body couples, is governed by [1]

$$\operatorname{div} \vec{u} = 0, \quad (2.1)$$

$$-(\mu + \kappa) \operatorname{curl} \operatorname{curl} \vec{u} + \kappa \operatorname{curl} \vec{v} - \operatorname{grad} p = 0, \quad (2.2)$$

$$(\alpha + \beta + \gamma) \operatorname{grad} \operatorname{div} \vec{v} - \gamma \operatorname{curl} \operatorname{curl} \vec{v} + \kappa \operatorname{curl} \vec{u} - 2\kappa \vec{v} = 0, \quad (2.3)$$

where \vec{u} , \vec{v} are representing the vectors of velocity and microrotation, and p denotes the pressure throughout the fluid flow. The physical constants (μ, κ) are characterizing the viscosity parameters and (α, β, γ) are denoting the gyro-viscosity coefficients. In the governing Eqs. (2.2)–(2.3), the assumption of low ($\ll 1$) Reynolds numbers is employed so that the non linear inertial terms have been neglected.

The following relations give the stress and couple stress tensors, respectively [1]

$$t_{ij} = -p\delta_{ij} + \mu(u_{j,i} + u_{i,j}) + \kappa(u_{j,i} - \varepsilon_{ijk}v_k), \quad (2.4)$$

$$m_{ij} = \alpha v_{r,r} \delta_{ij} + \beta v_{i,j} + \gamma v_{j,i}, \quad (2.5)$$

where δ_{ij} is denoting the Kronecker delta and ε_{ijk} is representing the alternating tensor.

3 Statement of the problem

Consider the slow steady rotational motion of an incompressible micropolar fluid past a rotating sphere of radius a with angular velocity Ω about a diameter perpendicular to an impermeable plane wall located at a distance b from the center of the particle, as shown in Fig. 1. It is convenient to choose the center of the sphere at the origin and to use cylindrical system of coordinates (ρ, ϕ, z) together with the spherical coordinates (r, θ, ϕ) . According to the axisymmetric nature of the problem, all the field functions do not depend on the coordinate ϕ and thus the vectors of the velocity and microrotation can be represented as follows

$$\vec{u} = u_\phi(\rho, z) \vec{e}_\phi, \quad (3.1)$$

$$\vec{v} = v_\rho(\rho, z) \vec{e}_\rho + v_z(\rho, z) \vec{e}_z, \quad (3.2)$$

Let

$$\text{div } \vec{v} = F, \quad \text{curl } \vec{v} = G \vec{e}_\phi, \quad (3.3)$$

The field Eqs. (2.2)–(2.3) reduce to

$$\frac{\partial p}{\partial \rho} = 0, \quad \frac{\partial p}{\partial z} = 0, \quad (3.4)$$

$$(\mu + \kappa)L_{-1}u_\phi + \kappa G = 0, \quad (3.5)$$

$$v_\rho = \frac{1}{\chi^2} \frac{\partial F}{\partial \rho} + \frac{\gamma}{2\kappa} \frac{\partial G}{\partial z} - \frac{1}{2} \frac{\partial u_\phi}{\partial z}, \quad (3.6)$$

$$v_z = \frac{1}{\chi^2} \frac{\partial F}{\partial z} - \frac{\gamma}{2\kappa} \frac{1}{\rho} \frac{\partial}{\partial \rho}(\rho G) + \frac{1}{2\rho} \frac{\partial}{\partial \rho}(\rho u_\phi), \quad (3.7)$$

where

$$\chi^2 = \frac{2\kappa}{\alpha + \beta + \gamma}.$$

Equation (3.4) implies that the pressure is constant throughout the flow. In addition, the velocity u_ϕ and the two functions F and G can be obtained by solving the differential equations

$$L_{-1}(L_{-1} - \ell^2)u_\phi = 0, \quad (3.8)$$

$$(\nabla^2 - \chi^2)F = 0, \quad (3.9)$$

$$(L_{-1} - \ell^2)G = 0, \quad (3.10)$$

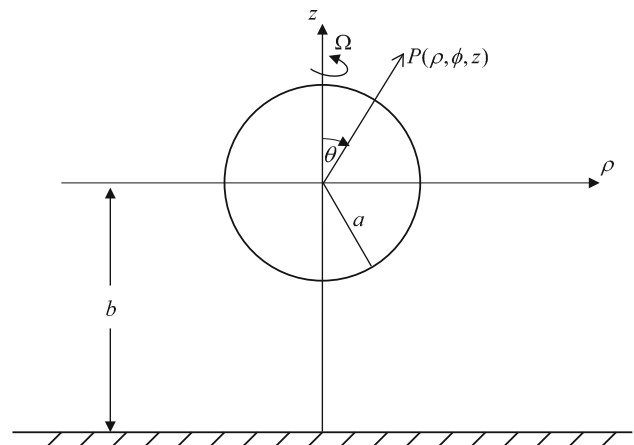
where

$$L_{-1} = \frac{\partial^2}{\partial \rho^2} - \frac{1}{\rho} \frac{\partial}{\partial \rho} + \frac{\partial^2}{\partial z^2}, \quad (3.11)$$

$$\ell^2 = \kappa(2\mu + \kappa)/\gamma(\mu + \kappa).$$

To complete the formulation of the problem, the boundary conditions have to be specified at the surface of the sphere and at the surface of the impermeable plane. In the present study, we propose the slip and spin boundary conditions at the surface of the sphere and the no-slip and no-spin conditions at the surface of the plane wall. It is of some interest to investigate the possibility that the macro-elements of the micropolar fluid may slip at the surface of the sphere. For

Fig. 1 Geometry of the problem



Newtonian fluids, this issue was first treated by Basset [24]. Therefore, based on the slip boundary condition of Newtonian fluids, the reasonable assumption of this condition for micropolar fluids is that the tangential velocity of the fluid relative to the solid at a point on its surface is proportional to the tangential stress of the fluid at that point. The constant of proportionality, β_1 , between these two quantities is called the coefficient of sliding friction. It is assumed to depend only on the nature of the fluid and solid surface. The slip condition is a dynamical boundary condition. We think that this boundary condition is a physically realistic condition to apply at slip surfaces for micropolar fluids. The second boundary condition that we will apply at the surface of the rotating sphere is a condition about the microrotation vector. It should be noted here that there is no uniform consensus on the microrotation boundary conditions for micropolar fluids. An interesting review for various types of this boundary condition is given by Migun [35]. Condiff and Dahler [36] proposed a kinematic boundary condition that relates the microrotation and vorticity vectors at the surface of the sphere. This condition is called the spin-vorticity condition which states that the microrotation is proportional to the vorticity. The constant of proportionality, s , between these two quantities is called the spin parameter. It depends also on the nature of the fluid and solid. Therefore at the surface of the rigid sphere, $r = a$

$$\beta_1(u_\phi - \rho \Omega) = \tau_{r\phi}, \quad (3.12)$$

$$\vec{v}|_{\text{boundary}} = \frac{s}{2} \text{curl } \vec{u}|_{\text{boundary}}, \quad (3.13)$$

where the coefficient β_1 varies between zero and infinity. If the slip coefficient is taken equal to zero, the case of perfect slip is then considered. In addition, the classical no-slip case can be recovered when the slip coefficient approaches infinity and a finite value of β_1 corresponds to a partial slip. The parameter s is varying from 0 to 1. The no-spin case corresponds to $s = 0$; that is the micro-elements close to the boundary are not able to rotate, and $s = 1$ corresponds to perfect spin of the microelements at the surface of the solid body. In fact, the dynamical slip boundary condition (3.12) is used by many authors in the literature for Newtonian viscous fluids. The slip length parameter μ/β_1 has been measured under various physical and geometrical circumferences for viscous fluids

[37–39]; and it is basically found that this parameter depends on the nature of fluid and solid. This motivated us to use the slip hypothesis for micropolar fluids.

On the plane wall, $z = -b$, we have

$$u_\phi = 0, \quad (3.14)$$

$$v_\rho = 0, \quad v_z = 0, \quad (3.15)$$

Also, far away from the particle, we have

$$u_\phi \rightarrow 0, \quad v_\rho \rightarrow 0, \quad v_z \rightarrow 0 \quad \text{as } r \rightarrow \infty. \quad (3.16)$$

4 Method of solution

We shall use the method of superposition to solve the problem. The solution of the problem will be taken as the sums of the solutions of two different problems. The first problem is similar to the current one with the absence of the wall. This one is solved using spherical polar coordinates. In the second problem we assume that the sphere is removed after reaching the steady state and solve the new problem of steady motion past the wall using cylindrical coordinates. Mathematically speaking, since the equations of motion and the boundary conditions characterizing the problem at hand are linear, then the superposition principle can be used such that [12–15]

$$u_\phi = u_{\phi s} + u_{\phi w}, \quad (4.1)$$

$$v_\rho = v_{\rho s} + v_{\rho w}, \quad (4.2)$$

$$v_z = v_{zs} + v_{zw}, \quad (4.3)$$

where the parts $u_{\phi s}$, $v_{\rho s}$, v_{zs} denote the general solution of the equations of motion in the spherical polar coordinate system (r, θ, ϕ) which give vanishing fluid velocity and vanishing microrotation components as $r \rightarrow \infty$. The parts $u_{\phi w}$, $v_{\rho w}$, v_{zw} represent the general solution of the equations of motion in the cylindrical system of coordinates (ρ, ϕ, z) which produce finite velocity and finite microrotation components everywhere in the flow field [12].

The general solutions of Eqs. (3.8) and (3.9) in spherical coordinates, which are regular as $r \rightarrow \infty$, are given respectively, by

$$u_{\phi s} = \sum_{n=1}^{\infty} \left(A_n r^{-n-1} + B_n r^{-1/2} K_{n+1/2}(\ell r) \right) P_n^1(\zeta); \zeta = \cos\theta, \tag{4.4}$$

$$F_s = - \sum_{n=1}^{\infty} C_n r^{-1/2} K_{n+1/2}(\chi r) P_n(\zeta), \tag{4.5}$$

where A_n, B_n, C_n are unknown constants.

Inserting the solution (4.4) into Eq. (3.5), we obtain

$$G_s = - \frac{\mu + \kappa}{\kappa} \ell^2 \sum_{n=1}^{\infty} B_n r^{-1/2} K_{n+1/2}(\ell r) P_n^1(\zeta). \tag{4.6}$$

Substituting expressions (4.4)–(4.6) into (3.6) and (3.7), we get the microrotation components as

$$v_{\rho s} = \sum_{n=1}^{\infty} [A_n A_{1n}(r, \zeta) + B_n B_{1n}(r, \zeta) + C_n C_{1n}(r, \zeta)], \tag{4.7}$$

$$v_{z s} = \sum_{n=1}^{\infty} [A_n A_{2n}(r, \zeta) + B_n B_{2n}(r, \zeta) + C_n C_{2n}(r, \zeta)]. \tag{4.8}$$

Moreover, the function given by the expression (4.4) can be rewritten as

$$u_{\phi s} = \sum_{n=1}^{\infty} [A_n A_{3n}(r, \zeta) + B_n B_{3n}(r, \zeta)], \tag{4.9}$$

where the functions $A_{in}, B_{in}, i = 1, 2, 3$ and $C_{jn}, j = 1, 2$ are listed in the ‘‘Appendix A’’.

The general solutions of the Stokes Eqs. (3.8) and (3.9) in the cylindrical coordinate system are given, respectively, by

$$u_{\phi w} = \int_0^{\infty} [A(w)e^{-\omega z} + B(w)e^{-\xi z}] \omega J_1(\omega \rho) d\omega, \tag{4.10}$$

$$F_w = \int_0^{\infty} C(\omega) e^{-\tau z} \omega J_0(\omega \rho) d\omega, \tag{4.11}$$

The integrals (4.10) and (4.11) rather than the infinite series form of the solution in cylindrical coordinates is required owing to the infinite non-periodic extent of the planar boundary. By proper choice of the unknown functions $A(w), B(w)$ and $C(w)$, the solutions (4.10) and (4.11) are capable of

exactly cancelling the disturbances produced by the sphere along the confining wall [12].

where $\xi = \sqrt{\omega^2 + \ell^2}, \tau = \sqrt{\omega^2 + \chi^2}$.

From (3.5) and (4.4), we have

$$G_w = - \frac{\mu + \kappa}{\kappa} \ell^2 \int_0^{\infty} B(\omega) \omega e^{-\xi z} J_1(\omega \rho) d\omega, \tag{4.12}$$

Substitution from (4.10)–(4.12) in (3.6) and (3.7) we get

$$v_{\rho w} = \int_0^{\infty} \left[\frac{1}{2} A(w) \omega^2 e^{-\omega z} + \frac{(\mu + \kappa)}{\kappa} B(w) \xi \omega e^{-\xi z} - \frac{C(w)}{\chi^2} \omega^2 e^{-\tau z} \right] J_1(\omega \rho) d\omega, \tag{4.13}$$

$$v_{z w} = \int_0^{\infty} \left[\frac{1}{2} A(w) \omega^2 e^{-\omega z} + \frac{(\mu + \kappa)}{\kappa} B(w) \omega^2 e^{-\xi z} - \frac{C(w)}{\chi^2} \tau \omega e^{-\tau z} \right] J_0(\omega \rho) d\omega \tag{4.14}$$

Substituting the above expressions into (4.1)–(4.3), we get the following expressions of the fluid velocity and microrotation components

$$v_{\rho} = \sum_{n=1}^{\infty} (A_n A_{1n}(\rho, z) + B_n B_{1n}(\rho, z) + C_n C_{1n}(\rho, z)) + \int_0^{\infty} L_1(\omega, z) \omega J_1(\omega \rho) d\omega, \tag{4.15}$$

$$v_z = \sum_{n=1}^{\infty} (A_n A_{2n}(\rho, z) + B_n B_{2n}(\rho, z) + C_n C_{2n}(\rho, z)) + \int_0^{\infty} L_2(\omega, z) \omega J_0(\omega \rho) d\omega, \tag{4.16}$$

$$u_{\phi} = \sum_{n=1}^{\infty} (A_n A_{3n}(\rho, z) + B_n B_{3n}(\rho, z)) + \int_0^{\infty} L_3(\omega, z) \omega J_1(\omega \rho) d\omega, \tag{4.17}$$

where the functions $L_i(\omega, z)$ with $i = 1, 2, 3$ are listed in the “Appendix A”.

The tangential stress component $\tau_{r\phi}$ is given by

$$\frac{\tau_{r\phi}}{2\mu + \kappa} = \sum_{n=2}^{\infty} (A_n \alpha_n(\rho, z) + B_n \beta_n(\rho, z) + C_n \gamma_n(\rho, z)) + \int_0^{\infty} (A(\omega)R + B(\omega)S + C(\omega)T) d\omega \tag{4.18}$$

where the functions $\alpha_n, \beta_n, \gamma_n$ and R, S, T are listed in the “Appendix A”

Applying the boundary conditions (3.14) and (3.15) on the surface of the plane wall $z = -b$ to Eqs. (4.15)–(4.17) we get

$$L_1(\omega, -b) = \sum_{n=1}^{\infty} (A_n A_{1n}^*(\omega, -b) + B_n B_{1n}^*(\omega, -b) + C_n C_{1n}^*(\omega, -b)), \tag{4.19}$$

$$L_2(\omega, -b) = \sum_{n=1}^{\infty} (A_n A_{2n}^*(\omega, -b) + B_n B_{2n}^*(\omega, -b) + C_n C_{2n}^*(\omega, -b)), \tag{4.20}$$

$$L_3(\omega, -b) = \sum_{n=1}^{\infty} (A_n A_{3n}^*(\omega, -b) + B_n B_{3n}^*(\omega, -b)), \tag{4.21}$$

where A_{in}^*, B_{in}^* and $C_{in}^*, i = 1, 2, 3$ are listed in the “Appendix B”.

Substituting the expressions (A.9)–(A.11) for $L_i(\omega, -b), i = 1, 2, 3$ into (4.19)–(4.21), we obtain a linear system of three algebraic equations that can be solved simultaneously to give the unknown functions $A(\omega), B(\omega)$ and $C(\omega)$ as follows

$$A(\omega) = \sum_{n=1}^{\infty} (A_n A_n^{(1)}(\omega) + B_n B_n^{(1)}(\omega) + C_n C_n^{(1)}(\omega)), \tag{4.22}$$

$$B(\omega) = \sum_{n=1}^{\infty} (A_n A_n^{(2)}(\omega) + B_n B_n^{(2)}(\omega) + C_n C_n^{(2)}(\omega)), \tag{4.23}$$

$$C(\omega) = \sum_{n=1}^{\infty} (A_n A_n^{(3)}(\omega) + B_n B_n^{(3)}(\omega) + C_n C_n^{(3)}(\omega)), \tag{4.24}$$

where the functions $A_n^{(i)}, B_n^{(i)}, C_n^{(i)}$ with $i = 1, 2, 3$ are listed in the “Appendix B”.

Substituting Eqs. (4.22)–(4.24) together with equations (A.9)–(A.11) into expressions (4.15)–(4.17), we get after some rearrangements the velocity and microrotation components

$$v_\rho = \sum_{n=1}^{\infty} (A_n (A_{1n} + A'_{1n}) + B_n (B_{1n} + B'_{1n}) + C_n (C_{1n} + C'_{1n})), \tag{4.25}$$

$$v_z = \sum_{n=1}^{\infty} (A_n (A_{2n} + A'_{2n}) + B_n (B_{2n} + B'_{2n}) + C_n (C_{2n} + C'_{2n})), \tag{4.26}$$

$$u_\phi = \sum_{n=1}^{\infty} (A_n (A_{3n} + A'_{3n}) + B_n (B_{3n} + B'_{3n}) + C_n C_{3n}'), \tag{4.27}$$

where $A'_{kn}, B'_{kn}, C'_{kn}, k = 1, 2, 3$ are listed in the “Appendix B”.

Inserting (4.22)–(4.24) into (4.18), we obtain the shear stress $\tau_{r\phi}$ in terms of A_n, B_n and C_n in the form

$$\frac{\tau_{r\phi}}{2\mu + \kappa} = \sum_{n=1}^{\infty} (A_n (\alpha_n(\rho, z) + \alpha'_n(\rho, z)) + B_n (\beta_n(\rho, z) + \beta'_n(\rho, z)) + C_n (\gamma_n(\rho, z) + \gamma'_n(\rho, z))), \tag{4.28}$$

where the functions $\alpha'_n, \beta'_n, \gamma'_n$ are listed in the “Appendix A”.

Now, we apply the remaining boundary conditions on the spherical boundary by substituting expressions (4.25)–(4.28) into Eqs. (3.12) and (3.13) to get

$$\sum_{n=1}^{\infty} A_n (A_{1n}(a, \theta) + A'_{1n}(a, \theta)) + B_n (B_{1n}(a, \theta) + B'_{1n}(a, \theta)) + C_n (C_{1n}(a, \theta) + C'_{1n}(a, \theta)) = 0, \tag{4.29}$$

$$\begin{aligned} &\sum_{n=1}^{\infty} A_n (A_{2n}(a, \theta) + A'_{2n}(a, \theta)) \\ &\quad + B_n (B_{2n}(a, \theta) + B'_{2n}(a, \theta)) \\ &\quad + C_n (C_{2n}(a, \theta) + C'_{2n}(a, \theta)) \\ &= \Omega s, \end{aligned} \tag{4.30}$$

$$\begin{aligned} &\sum_{n=1}^{\infty} A_n ((A_{3n}(a, \theta) + A'_{3n}(a, \theta)) - \lambda_0 (\alpha_n(a, \theta) + \alpha'_n(a, \theta))) \\ &\quad + B_n ((B_{3n}(a, \theta) + B'_{3n}(a, \theta)) - \lambda_0 (\beta_n(a, \theta) + \beta'_n(a, \theta))) \\ &\quad + C_n ((C_{3n}(a, \theta) + C'_{3n}(a, \theta)) - \lambda_0 (\gamma_n(a, \theta) + \gamma'_n(a, \theta))) \\ &= a\Omega s \sin \theta, \end{aligned} \tag{4.31}$$

where $\lambda_0 = (2 + \kappa/\mu)\lambda$ is the non-dimensional slip parameter on the spherical boundary and $\lambda = \mu/a\beta_1$.

The total couple, $T_z \vec{e}_z$, acting on an axi-symmetrical particle, rotating about its axis of revolution in a micropolar fluid can be obtained by applying the formula [2]

$$T_z = 4\pi (2\mu + \kappa) \lim_{r \rightarrow \infty} \frac{r^2 u_\phi}{\sqrt{1 - \zeta^2}}, \tag{4.32}$$

Applying this formula to the problem at hand, we get the hydrodynamic couple acting on the surface of the sphere as

$$T_z = 4\pi (2\mu + \kappa) A_1. \tag{4.33}$$

The boundary collocation method is used to determine the unknown constants A_n, B_n, C_n numerically. To satisfy the conditions applied in Eqs. (4.29)–(4.31) along the entire spherical surface we use the collocation method. The collocation technique enforces the imposed conditions at a finite number of discrete points on the generating arc of the spherical particle (from $\theta = 0$ to π) and then truncating the infinite series in Eqs. (4.25)–(4.28) into finite ones. Satisfying the boundary conditions (3.12) and (3.13) at N discrete points on the generating arc of the spherical boundary, thus the infinite series in Eqs. (4.25)–(4.28) are truncated after N terms. This results in a system of $3N$ linear algebraic equations in the truncated form of (4.29)–(4.31) that can be solved simultaneously to give the $3N$ unknown constants A_n, B_n and C_n . The fluid velocity and microrotation components are then obtained. The definite integrals appearing in Eqs. (4.29)–(4.31) (see “Appendix A”) are performed numerically. To improve the accuracy

of the truncation technique to any degree, we can take a sufficiently large value of N .

5 Results and discussion

The arc $0 \leq \theta \leq \pi$ was divided into N equal parts by the points $\theta_1 = \delta, \theta_k = k/\pi, k = 2, 3, \dots, N-1, \theta_N = \pi - \delta$, where δ is a small positive number. As mentioned before, substitution of these values in the boundary conditions gives us a system of $3N$ linear equations. These equations were solved numerically using a Fortran program utilizing the LU-decomposition method. We started with $N = 5$ and increased N in steps of 5. Watching the resulting values, we found that for $N \leq 40$ the values have stabilized up to 4 decimal places. In all the calculations of this manuscript and other manuscripts by the authors [4, 26, 34] it was found that the resulting matrix is always invertible. This is not always the case. It was reported in [40] that in some rare cases counter examples can be constructed.

The collocation solutions of the non-dimensional hydrodynamic couple, $\tilde{T} = T_z/a^3\mu\Omega$, on the solid sphere caused by the surrounding fluid for different values of the parameters $a/b, 1/\lambda, \kappa/\mu$ and s are tabulated in Tables 1 and 2 and graphed in Figs. 2 and 3. For small values of the aspect ratio a/b , the number of collocation points needed is less than 20 while for larger values of the aspect ratio the number of collocation points reached 40. As expected, the results in Table 1 indicate that the non-dimensional couple increases monotonically with the increase of κ/μ , for any given value of the ratio $a/b > 0.01$. It also shows that, for any given value of κ/μ , the couple increases monotonically with the increase of a/b . It can be concluded from this table that the couple values decreases considerably as the aspect ratio becomes smaller. It can be expected also that the couple vanishes when the aspect ratio a/b is taken zero. In addition, the results presented in Table 1 agree with the results of Wan and Keh [41] for classical viscous fluids when the micropolarity parameter κ/μ vanishes.

The results tabulated in Table 2 illustrate that the non-dimensional couple is monotonically increasing function of s , for any given value of ratio a/b . Figures 2 and 3 shows the behavior of the non-dimensional couple versus $1/\lambda$ for different values of

Table 1 The normalized couple for different values of the diameter ratio a/b and different values of the micropolarity ratio κ/μ when $1/\lambda = 10$ and $s = 0.1$

a/b	N	\tilde{T}				
		$\kappa/\mu = 0$	$\kappa/\mu = 1$	$\kappa/\mu = 2$	$\kappa/\mu = 4$	$\kappa/\mu = 6$
0.01	10	0.0000	0.0026	0.0048	0.0040	0.0042
	15	0.0000	0.0046	0.0047	0.0047	0.0047
	20	0.0000	0.0046	0.0047	0.0047	0.0047
0.1	10	0.0063	0.0615	0.0650	0.0702	0.0740
	15	0.0063	0.0613	0.0652	0.0702	0.0740
	20	0.0063	0.0613	0.0652	0.0702	0.0740
0.3	10	0.3387	0.6212	0.6965	0.7883	0.8510
	15	0.3387	0.6213	0.6965	0.7903	0.8529
	20	0.3387	0.6213	0.6965	0.7903	0.8529
0.5	30	1.9445	2.8942	3.3539	3.9556	4.3523
	35	1.9445	2.8944	3.3539	3.9558	4.3525
	40	1.9445	2.8944	3.3539	3.9558	4.3525
0.7	30	5.8603	8.3147	9.8733	12.0681	13.5755
	35	5.8603	8.3147	9.8747	12.0683	13.5756
	40	5.8603	8.3147	9.8747	12.0683	13.5756
0.9	30	12.8997	18.0271	21.7781	27.3969	31.4664
	35	12.8997	18.0277	21.7792	27.3977	31.4674
	40	12.8997	18.0277	21.7792	27.3977	31.4674

the aspect ratio a/b and the spin parameter, respectively. It is observed that the values of the couple increases with the increase of the slip parameter. The case of classical no slip condition is reached when the slip parameter $1/\lambda$ approaches infinity while the case of perfect slip is obtained when the slip parameter is assigned the value zero. It can be concluded also from the tables that in the limiting case when the aspect ratio a/b approaches zero, the torque acting on the sphere vanishes; that is the sphere itself will disappear.

6 Conclusion

The motion of a spherical particle rotating steadily in a micropolar fluid about a diameter perpendicular to an infinite plane wall is investigated theoretically. A semi analytical technique together with the numerical collocation method has been utilized to obtain the solution of the equations of motion characterizing the slow steady motion of a micropolar fluid. It is assumed that the fluid particles close to the rigid spherical boundary can slip and spin while the no-slip and no-spin conditions are imposed on the surface of the plane wall. The total couple experienced by the fluid on the

particle is obtained. One of the important results of this problem is that the spin parameter has a significant influence on the couple acting on the spherical particle. In addition, the increase of the micropolarity parameter increases the resistance of the micropolar fluid so that the values of the couple experienced by the fluid increase. It is observed from the numerical results that the aspect ratio a/b plays an important role in choosing the number of collocation points.

Compliance with ethical standards

Conflicts of interest The authors declare that they have no conflict of interest.

Appendix A

$$A_{1n} = \frac{r^{-n-2}}{2} [(2n + 1)\zeta P_n^1(\zeta) - (n + 1)P_{n-1}^1(\zeta)], \tag{A.1}$$

$$B_{1n} = \frac{(\mu + \kappa)}{\kappa} \left[-(n + 1)r^{-3/2} K_{n+1/2}(\ell r) P_{n-1}^1(\zeta) + \ell \zeta r^{-1/2} K_{n+3/2}(\ell r) P_n^1(\zeta) \right], \tag{A.2}$$

Table 2 The normalized couple for different values of the diameter ratio a/b and different values of the spin parameter s for $1/\lambda = 10$ and $\kappa/\mu = 2$

a/b	N	\tilde{T}			
		$s = 0$	$s = 0.1$	$s = 0.5$	$s = 1.0$
0.01	10	0.0000	0.0048	0.0238	0.0476
	15	0.0000	0.0047	0.0233	0.0465
	20	0.0000	0.0047	0.0233	0.0465
0.1	10	0.0069	0.0650	0.2975	0.5880
	15	0.0069	0.0652	0.2981	0.5893
	20	0.0069	0.0652	0.2981	0.5893
0.3	10	0.4465	0.6965	1.6962	2.9463
	15	0.4465	0.6965	1.6965	2.9466
	20	0.4465	0.6965	1.6965	2.9466
0.5	30	2.8271	3.3539	5.4611	8.0950
	35	2.8271	3.3539	5.4613	8.0955
	40	2.8271	3.3539	5.4613	8.0955
0.7	30	9.0336	9.8733	13.2363	17.4413
	35	9.0340	9.8747	13.2379	17.4417
	40	9.0340	9.8747	13.2379	17.4417
0.9	30	20.6980	21.7781	26.1011	31.5076
	35	20.6982	21.7792	26.1033	31.5084
	40	20.6982	21.7792	26.1033	31.5084

$$C_{1n} = \frac{1}{\chi^2 \sqrt{1 - \zeta^2}} \left\{ nr^{-3/2} K_{n+1/2}(\chi r) (\zeta P_{n-1}(\zeta) - P_n(\zeta)) + \chi r^{-1/2} (1 - \zeta^2) K_{n+3/2}(\chi r) P_n(\zeta) \right\} \tag{A.3}$$

$$A_{2n} = \frac{r^{-n-2}}{2\sqrt{1 - \zeta^2}} \left[((2n + 1)\zeta^2 - n) P_n^1(\zeta) - (n + 1)\zeta P_{n-1}^1(\zeta) \right], \tag{A.4}$$

$$B_{2n} = \frac{(\mu + \kappa)}{\kappa \sqrt{1 - \zeta^2}} B_n \left\{ (n + 1) r^{-3/2} K_{n+1/2}(\ell r) (P_n^1(\zeta) - \zeta P_{n-1}^1(\zeta)) - \ell (1 - \zeta^2) r^{-1/2} K_{n+3/2}(\ell r) P_n^1(\zeta) \right\} \tag{A.5}$$

$$C_{2n} = \frac{1}{\chi^2} \left[-nr^{-3/2} K_{n+1/2}(\chi r) P_{n-1}(\zeta) + \chi \zeta r^{-1/2} K_{n+3/2}(\chi r) P_n(\zeta) \right], \tag{A.6}$$

$$A_{3n} = \frac{nr^{-n-1}}{\sqrt{1 - \zeta^2}} [P_{n-1}(\zeta) - \zeta P_n(\zeta)], \tag{A.7}$$

Fig. 2 Variations of the normalized couple versus slip parameter for different values of κ/μ when $a/b = 0.2$ and $s = 0.1$

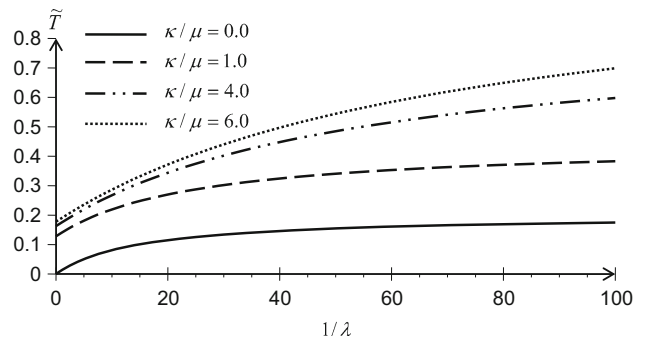
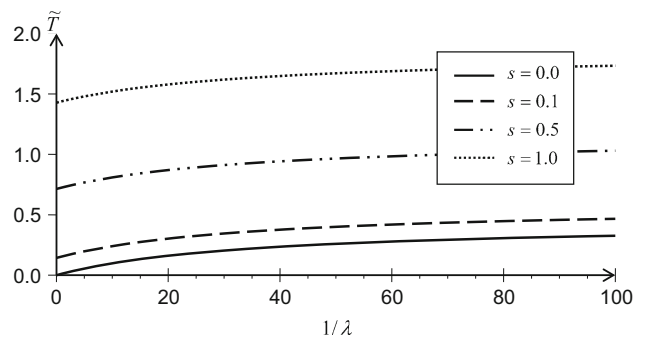


Fig. 3 Variations of the normalized couple versus slip parameter for different values of the spin parameter when $a/b = 0.2$ and $\kappa/\mu = 2$



$$B_{3n} = \frac{n}{\sqrt{1-\zeta^2}} r^{-1/2} K_{n+1/2}(\ell r) [P_{n-1}(\zeta) - \zeta P_n(\zeta)], \tag{A.8}$$

$$L_1(\omega, z) = \left[\frac{1}{2} A(\omega) \omega e^{-\omega z} + \frac{(\mu + \kappa)}{\kappa} B(\omega) \zeta e^{-\zeta z} - \frac{C(\omega)}{\chi^2} \omega e^{-\tau z} \right], \tag{A.9}$$

$$L_2(\omega, z) = \left[\frac{1}{2} A(\omega) \omega e^{-\omega z} + \frac{(\mu + \kappa)}{\kappa} B(\omega) \omega e^{-\zeta z} - \frac{C(\omega)}{\chi^2} \tau e^{-\tau z} \right], \tag{A.10}$$

$$L_3(\omega, z) = (A(\omega) e^{-\omega z} + B(\omega) e^{-\zeta z}), \tag{A.11}$$

$$\alpha_n(r, \zeta) = -\frac{n(2+n)}{2\sqrt{1-\zeta^2}} r^{-n-2} [P_{n-1}(\zeta) - \zeta P_n(\zeta)], \tag{A.12}$$

$$\beta_n(r, \zeta) = -\frac{nr^{-3/2}}{\sqrt{1-\zeta^2}} K_{n+1/2}(\ell r) [P_{n-1}(\zeta) - \zeta P_n(\zeta)], \tag{A.13}$$

$$\gamma_n(r, \zeta) = \frac{\kappa nr^{-3/2}}{\chi^2(2\mu + \kappa)\sqrt{1-\zeta^2}} K_{n+1/2}(\chi r) [P_{n-1}(\zeta) - \zeta P_n(\zeta)], \tag{A.14}$$

$$R = \left[\frac{1}{2} \omega e^{-\omega z} (\omega \sin \theta J_0(\omega \rho) - (\omega z + 2)r^{-1} J_1(\omega \rho)) \right] \tag{A.15}$$

$$S = -[\omega r^{-1} e^{-\zeta z} J_1(\omega \rho)], \tag{A.16}$$

$$T = \left[\frac{\kappa \omega}{\chi^2(2\mu + \kappa)} e^{-\tau z} (\tau \sin \theta J_0(\omega \rho) - \omega \cos \theta J_1(\omega \rho)) \right]. \tag{A.17}$$

Appendix B

We can show by induction that

$$\int_0^\infty \frac{n(n+1)}{2} \varpi^{-n-1} \left[P_n\left(\frac{-b}{\varpi}\right) + \frac{b}{\varpi} P_{n+1}\left(\frac{-b}{\varpi}\right) \right] J_1(\rho \omega) d\rho = \frac{(-1)^n \omega^n b^n}{2(n-1)!} e^{-b\omega}, \tag{B.1}$$

$$\begin{aligned} n(n+1) \int_0^\infty \frac{1}{\sqrt{\varpi}} \left[\ell z K_{n+3/2}(\ell \varpi) G_{n+1}\left(\frac{-b}{\varpi}\right) - (n-1) K_{n+1/2}(\ell r) G_n\left(\frac{-b}{\varpi}\right) \right] J_1(\rho \omega) d\rho \\ = (-1)^n n(n+1) \sqrt{\frac{\pi}{2}} \frac{\sqrt{\ell}}{\omega} e^{-b\zeta} G_{n+1}\left(\frac{\zeta}{\ell}\right), \end{aligned} \tag{B.2}$$

$$\begin{aligned} \int_0^\infty \frac{1}{\sqrt{\varpi}} \left[\frac{-n K_{n+1/2}(\chi r)}{\chi^2} \left[P_n\left(\frac{-b}{\varpi}\right) - \frac{-b}{\varpi} P_{n-1}\left(\frac{-b}{\varpi}\right) \right] + \frac{1}{\chi} \sqrt{\varpi} (1-\zeta^2) K_{n+3/2}(\chi r) P_n\left(\frac{-b}{\varpi}\right) \right] J_1(\omega \rho) d\rho \\ = (-1)^n \sqrt{\frac{\pi}{2}} \frac{\omega}{\tau} \chi^{-5/2} e^{-b\tau} P_n\left(\frac{\tau}{\chi}\right), \end{aligned} \tag{B.3}$$

where $\tau = \sqrt{\chi^2 + \omega^2}$, $\varpi = \sqrt{b^2 + \rho^2}$.

$$\begin{aligned} \int_0^\infty \frac{n(n+1)}{2} \varpi^{-n-2} P_{n+1}\left(\frac{-b}{\varpi}\right) \rho J_0(\rho \omega) d\rho \\ = \frac{(-1)^{n-1} \omega^n b^n}{2(n-1)!} e^{-\omega}, \end{aligned} \tag{B.4}$$

$$\begin{aligned} \int_0^\infty n(n+1) \left[r^{-3/2} K_{n+1/2}(\ell r) P_{n+1}\left(\frac{-b}{\varpi}\right) - \ell r^{-1/2} K_{n-1/2}(\ell r) G_{n+1}\left(\frac{-b}{\varpi}\right) \right] \rho J_0(\rho \omega) d\rho \\ = (-1)^{n-1} n(n+1) b \omega \sqrt{\frac{\pi}{2}} \frac{\sqrt{\ell}}{\zeta} e^{-b\zeta} G_{n+1}\left(\frac{\zeta}{\ell}\right), \end{aligned} \tag{B.5}$$

$$\begin{aligned} \int_0^\infty \frac{\rho r^{-3/2}}{\chi^2} \left[-n P_{n-1}\left(\frac{-b}{\varpi}\right) K_{n+1/2}(\chi r) + \chi z K_{n+3/2}(\chi r) P_n\left(\frac{-b}{\varpi}\right) \right] J_0(\rho \omega) d\rho \\ = -(-1)^n \sqrt{\frac{\pi}{2}} \chi^{-5/2} e^{-b\tau} P_n\left(\frac{\tau}{\chi}\right), \end{aligned} \tag{B.6}$$

$$\begin{aligned} & \int_0^\infty n\varpi^{-n} \left[P_{n-1} \left(\frac{-b}{\varpi} \right) + \frac{1}{\varpi} P_n \left(\frac{-b}{\varpi} \right) \right] J_1(\rho\omega) d\rho \\ &= \int_0^\infty n(n+1)\varpi^{-n} G_{n+1} \left(\frac{-b}{\varpi} \right) J_1(\rho\omega) d\rho \\ &= (-1)^{n-1} \frac{(b\omega)^{n-1}}{(n-1)!} e^{-b\omega}, \end{aligned} \tag{B.7}$$

$$\begin{aligned} & \int_0^\infty n\sqrt{\varpi} K_{n+1/2}(\ell\varpi) \left[P_{n-1} \left(\frac{-b}{\varpi} \right) + \frac{b}{\varpi} P_n \left(\frac{-b}{\varpi} \right) \right] J_1(\rho\omega) d\rho \\ &= \int_0^\infty n(n+1)\sqrt{\varpi} K_{n+1/2}(\ell\varpi) G_{n+1} \left(\frac{-b}{\xi} \right) J_1(\rho\omega) d\rho \\ &= (-1)^n n(n+1) \sqrt{\frac{\pi\sqrt{\ell}}{2\xi}} e^{-b\xi} G_{n+1} \left(\sqrt{1 + \left(\frac{\omega}{\ell}\right)^2} \right), \end{aligned} \tag{B.8}$$

Direct application of these integrals, we get

$$A_{1n}^*(\omega, -b) = \frac{(-1)^n \omega^n b^n}{2(n-1)!} e^{-b\omega}, \tag{B.9}$$

$$B_{1n}^*(\omega, -b) = (-1)^n n(n+1) \sqrt{\frac{\pi\sqrt{\ell}}{2\omega}} e^{-b\xi} G_{n+1} \left(\frac{\xi}{\ell} \right), \tag{B.10}$$

$$C_{1n}^*(\omega, -b) = (-1)^n \sqrt{\frac{\pi\omega}{2\tau}} \chi^{-5/2} e^{-b\tau} P_n \left(\frac{\tau}{\chi} \right), \tag{B.11}$$

$$A_{2n}^*(\omega, -b) = \frac{(-1)^{n-1} \omega^n b^n}{2(n-1)!} e^{-b\omega}, \tag{B.12}$$

$$B_{2n}^*(\omega, -b) = (-1)^{n-1} n(n+1) b\omega \sqrt{\frac{\pi\sqrt{\ell}}{2\xi}} e^{-b\xi} G_{n+1} \left(\frac{\xi}{\ell} \right), \tag{B.13}$$

$$C_{2n}^*(\omega, -b) = -(-1)^n \sqrt{\frac{\pi}{2}} \chi^{-5/2} e^{-b\tau} P_n \left(\frac{\tau}{\chi} \right), \tag{B.14}$$

$$A_{3n}^*(\omega, -b) = (-1)^{n-1} \frac{(b\omega)^{n-1}}{(n-1)!} e^{-b\omega}, \tag{B.15}$$

$$B_{3n}^*(\omega, -b) = -(-1)^n n(n+1) \sqrt{\frac{\pi\sqrt{\ell}}{2\xi}} e^{-b\xi} G_{n+1} \left(\frac{\xi}{\ell} \right). \tag{B.16}$$

Also

$$A_n^{(1)} = \frac{2e^{-b\omega}}{\Delta} \left[\tau \frac{\kappa}{\mu} A_{1n}^* - \frac{\kappa}{\mu} \omega A_{1n}^* + \left(1 + \frac{\kappa}{\mu} \right) (\omega^2 - \xi\tau) A_{1n}^* \right], \tag{B.17}$$

$$B_n^{(1)} = \frac{2e^{-b\omega}}{\Delta} \left[\tau \frac{\kappa}{\mu} B_{1n}^* - \frac{\kappa}{\mu} \omega B_{1n}^* + \left(1 + \frac{\kappa}{\mu} \right) (\omega^2 - \xi\tau) B_{1n}^* \right], \tag{B.18}$$

$$C_n^{(1)} = \frac{2e^{-b\omega}}{\Delta} \left[\tau \frac{\kappa}{\mu} C_{1n}^* - \frac{\kappa}{\mu} \omega C_{1n}^* \right], \tag{B.19}$$

$$A_n^{(2)} = -\frac{\kappa e^{-b\xi}}{\mu\Delta} \left[2\tau A_{1n}^* - 2\omega A_{2n}^* + \omega(\omega - \tau) A_{3n}^* \right], \tag{B.20}$$

$$B_n^{(2)} = -\frac{\kappa e^{-b\xi}}{\mu\Delta} \left[2\tau B_{1n}^* - 2\omega B_{2n}^* + \omega(\omega - \tau) B_{3n}^* \right], \tag{B.21}$$

$$C_n^{(2)} = -\frac{\kappa e^{-b\xi}}{\mu\Delta} \left[2\tau C_{1n}^* - 2\omega C_{2n}^* \right], \tag{B.22}$$

$$\begin{aligned} A_n^{(3)} &= \frac{e^{-b\tau}}{\Delta} \chi^2 \left\{ -\left(2 + \frac{\kappa}{\mu} \right) \omega A_{1n}^* \right. \\ &\quad \left. + \left(2\xi\kappa\mu^{-1} + 2\xi - \omega \frac{\kappa}{\mu} \right) A_{2n}^* \right. \\ &\quad \left. + \omega \left(1 + \frac{\kappa}{\mu} \right) (\omega - \xi) A_{3n}^* \right\}, \end{aligned} \tag{B.23}$$

$$\begin{aligned} B_n^{(3)} &= \frac{e^{-b\tau}}{\Delta} \chi^2 \left\{ -\left(2 + \frac{\kappa}{\mu} \right) \omega B_{1n}^* \right. \\ &\quad \left. + \left(2\xi \frac{\kappa}{\mu} + 2\xi - \omega \frac{\kappa}{\mu} \right) B_{2n}^* \right. \\ &\quad \left. + \omega \left(1 + \frac{\kappa}{\mu} \right) (\omega - \xi) B_{3n}^* \right\}, \end{aligned} \tag{B.24}$$

$$\begin{aligned} C_n^{(3)} &= \frac{e^{-b\tau}}{\Delta} \chi^2 \left[-\left(2 + \frac{\kappa}{\mu} \right) \omega C_{1n}^* \right. \\ &\quad \left. + \left(2\xi \frac{\kappa}{\mu} + 2\xi - \omega \frac{\kappa}{\mu} \right) C_{2n}^* \right], \end{aligned} \tag{B.25}$$

$$\Delta = \frac{\kappa}{\mu}(\omega^2 + \omega\tau - 2\xi\tau) + 2(\omega^2 - \xi\tau), \quad (\text{B.26})$$

$$A'_{1n}(r, \theta) = \int_0^\infty \left(\frac{1}{2} A_n^{(1)} \omega e^{-\omega z} + \frac{(\mu + \kappa)}{\kappa} A_n^{(2)} \xi e^{-\xi z} - \frac{A_n^{(3)}}{\chi^2} \omega e^{-\tau z} \right) \omega J_1(\omega\rho) d\omega, \quad (\text{B.27})$$

$$B'_{1n}(r, \theta) = \int_0^\infty \left(\frac{1}{2} B_n^{(1)} \omega e^{-\omega z} + \frac{(\mu + \kappa)}{\kappa} B_n^{(2)} \xi e^{-\xi z} - \frac{B_n^{(3)}}{\chi^2} \omega e^{-\tau z} \right) \omega J_1(\omega\rho) d\omega, \quad (\text{B.28})$$

$$C'_{1n}(r, \theta) = \int_0^\infty \left(\frac{1}{2} C_n^{(1)} \omega e^{-\omega z} + \frac{(\mu + \kappa)}{\kappa} C_n^{(2)} \xi e^{-\xi z} - \frac{C_n^{(3)}}{\chi^2} \omega e^{-\tau z} \right) \omega J_1(\omega\rho) d\omega, \quad (\text{B.29})$$

$$A'_{2n}(r, \theta) = \int_0^\infty \left(\frac{1}{2} A_n^{(1)} \omega e^{-\omega z} + \frac{(\mu + \kappa)}{\kappa} A_n^{(2)} \omega e^{-\xi z} - \frac{A_n^{(3)}}{\chi^2} \tau e^{-\tau z} \right) \omega J_0(\omega\rho) d\omega, \quad (\text{B.30})$$

$$B'_{2n}(r, \theta) = \int_0^\infty \left(\frac{1}{2} B_n^{(1)} \omega e^{-\omega z} + \frac{(\mu + \kappa)}{\kappa} B_n^{(2)} \omega e^{-\xi z} - \frac{B_n^{(3)}}{\chi^2} \tau e^{-\tau z} \right) \omega J_0(\omega\rho) d\omega, \quad (\text{B.31})$$

$$C'_{2n}(r, \theta) = \int_0^\infty \left(\frac{1}{2} C_n^{(1)} \omega e^{-\omega z} + \frac{(\mu + \kappa)}{\kappa} C_n^{(2)} \omega e^{-\xi z} - \frac{C_n^{(3)}}{\chi^2} \tau e^{-\tau z} \right) \omega J_0(\omega\rho) d\omega, \quad (\text{B.32})$$

$$A'_{3n}(r, \theta) = \int_0^\infty \left(A_n^{(1)} e^{-\omega z} + A_n^{(2)} e^{-\xi z} \right) \omega J_1(\omega\rho) d\omega, \quad (\text{B.33})$$

$$B'_{3n}(r, \theta) = \int_0^\infty \left(B_n^{(1)} e^{-\omega z} + B_n^{(2)} e^{-\xi z} \right) \omega J_1(\omega\rho) d\omega, \quad (\text{B.34})$$

$$C'_{3n}(r, \theta) = \int_0^\infty \left(C_n^{(1)} e^{-\omega z} + C_n^{(2)} e^{-\xi z} \right) \omega J_1(\omega\rho) d\omega, \quad (\text{B.35})$$

$$\alpha'_n(r, \theta) = \int_0^\infty \left(A_n^{(1)} R + A_n^{(2)} S + A_n^{(3)} T \right) d\omega, \quad (\text{B.36})$$

$$\beta'_n(r, \theta) = \int_0^\infty \left(B_n^{(1)} R + B_n^{(2)} S + B_n^{(3)} T \right) d\omega, \quad (\text{B.37})$$

$$\gamma'_n(r, \theta) = \int_0^\infty \left(C_n^{(1)} R + C_n^{(2)} S + C_n^{(3)} T \right) d\omega. \quad (\text{B.38})$$

References

1. Eringen AC (1998) *Microcontinuum field theories I and II*. Springer, New York
2. Ramkissoon H (1977) Slow steady rotation of an axially symmetric body in a micropolar fluid. *Appl Sci Res* 33:243–257
3. Charya DS, Iyengar TKV (2001) Rotary oscillations of an approximate sphere in an incompressible micropolar fluid. *Ind J Math* 43:129–144
4. Sherief HH, Faltas MS, Ashmawy EA (2010) Axi-symmetric translational motion of an arbitrary solid prolate body in a micropolar fluid. *Fluid Dyn Res* 42:065504-1-18
5. Kanwal RP (1960) Slow steady rotation of axially symmetric bodies in a viscous fluid. *J Fluid Mech* 10:17–24
6. O'Neill ME, Stewartson K (1967) On the slow motion of a sphere parallel to a near by wall. *J Fluid Mech* 27:705–724
7. Goldman AJ, Cox RG, Brenner H (1967) Slow viscous motion of a sphere parallel to a plane wall—I Motion through a quiescent fluid. *Chem Eng Sci* 22:637–651
8. Goldman AJ, Cox RG, Brenner H (1967) Slow viscous motion of a sphere parallel to a plane wall—II Couette flow. *Chem Eng Sci* 22:653–660

9. Gluckman MJ, Pfeffer R, Weinbaum S (1971) A new technique for treating multiparticle slow viscous flow: axisymmetric flow past spheres and spheroids. *J Math Mech* 50:705–740
10. Leichtberg S, Pfeffer R, Weinbaum S (1976) Stokes flow past finite coaxial clusters of spheres in a circular cylinder. *Int J Multiph Flow* 3:147–169
11. Kolodziej JA (1987) Review of application of boundary collocation methods in mechanics of continuous media. *Solid Mech Arch* 12:187–231
12. Ganatos P, Weinbaum S, Pfeffer R (1980) A strong interaction theory for the creeping motion of a sphere between plane parallel boundaries. Part 1. Perpendicular motion. *J Fluid Mech* 99:739–753
13. Keh HJ, Chang YC (2006) Slow motion of a slip spherical particle perpendicular to two plane walls. *J Fluids Struct* 22:647–661
14. Keh HJ, Hsu FC (2005) Photophoresis of an aerosol sphere normal to a plane wall. *J Colloid Interface Sci* 289:94–103
15. Kucaba-Piętal A (1999) Flow past a sphere moving towards a wall in micropolar fluid. *J Theor Appl Mech* 37:301–318
16. Kennard EH (1938) *Kinetic theory of gases*. McGraw-Hill, New York
17. Hutchins DK, Harper MH, Felder RL (1995) Slip correction measurements for solid spherical particles by modulated dynamic light scattering. *Aerosol Sci Technol* 22:202–218
18. Thompson A, Troian SM (1997) A general boundary condition for liquid flow at solid surfaces. *Nature* 389:360–362
19. Hocking LM (1976) A moving fluid interface on a rough surface. *J Fluid Mech* 76:801–817
20. Dussan EB (1979) On the spreading of liquids on solid surfaces: static and dynamic contact lines. *Annu Rev Fluid Mech* 11:371–400
21. Koplik J, Banavar JR (1995) Corner flow in the sliding plate problem. *Phys Fluids* 7:3118–3125
22. Richardson S (1973) On the no-slip boundary condition. *J Fluid Mech* 59:707–719
23. Navier CLMH (1823) *Memoirs de l'Academie Royale des Sciences de l'Institut de France* 1:414–416
24. Basset AB (1961) *A treatise on hydrodynamics*. Dover, New York
25. Sherief HH, Faltas MS, Ashmawy EA (2012) Stokes flow between two confocal rotating spheroids with slip. *Arch Appl Mech* 82:937–948
26. Ashmawy EA (2011) Slip at the surface of a general axisymmetric body rotating in a viscous fluid. *Arch Mech* 63(4):341–361
27. Neto C, Evans DR, Bonaccorso E, Butt H-J, Craig VSJ (2005) Boundary slip in Newtonian liquids: a review of experimental studies. *Rep Progr Phys* 68:2859–2897
28. Willmott G (2008) Dynamics of a sphere with inhomogeneous slip boundary conditions in Stokes flow. *Phys Rev E* 77:055302-1-4
29. Suna H, Liu C (2010) The slip boundary condition in the dynamics of solid particles immersed in Stokesian flows. *Solid State Commun* 150:990–1002
30. Yang F (2010) Slip boundary condition for viscous flow over solid surfaces. *Chem Eng Commun* 197:544–550
31. Ashmawy EA (2015) Fully developed natural convective micropolar fluid flow in a vertical channel with slip. *J Egypt Math Soc* 23:563–567
32. Sherief HH, Faltas MS, Ashmawy EA (2009) Galerkin representations and fundamental solutions for an axisymmetric microstretch fluid flow. *J Fluid Mech* 619:277–293
33. Ashmawy EA (2012) Unsteady Couette flow of a micropolar fluid with slip. *Meccanica* 47:85–94
34. Sherief HH, Faltas MS, Ashmawy EA, Nashwan MG (2014) Slow motion of a slip spherical particle along the axis of a circular cylindrical pore in a micropolar fluid. *J Mol Liq* 200:273–282
35. Migun NP (1984) On hydrodynamic boundary conditions for microstructural fluids. *Rheol Acta* 23:575–581
36. Condiff DW, Dahler JS (1964) Fluid mechanics aspects of antisymmetric stress. *Phys Fluids* 7:842–854
37. Trethewey DC, Meinhart CD (2002) Apparent fluid slip at hydrophobic microchannel walls. *Phys Fluids* 14:L9–L12
38. Trethewey DC, Meinhart CD (2004) A generating mechanism for apparent fluid slip in hydrophobic microchannels. *Phys Fluids* 16:1509–1515
39. Lauga E, Brenner MP, Stone HA (2007) Microfluidics: the no-slip boundary condition. In: Foss J, Tropea C, Yarin A (eds) *Handbook of experimental fluid dynamics*. Springer, Berlin, pp 1219–1240
40. Pearson JW (2011) A radial basis function method for solving PDE constrained optimization problems, Oxford University Mathematical Institute, Numerical Analysis Group, Report no. 11/06
41. Wan YW, Keh HJ (2011) Slow rotation of an axially symmetric particle about its axis of revolution normal to one or two plane walls. *CMES* 74:109–137